Table 1
Demographics and characteristics of cases

Number	Age (years)	Gender	PMT (h:min)	NFT[a]	Senile plaque
1	52	M	15:51	0	0
2	69	F	11:48	0	A
3	82	F	39:04	0	0
4	87	M	70:10	0	0
5	78	M	2:02	0	0
6	66	F	9:51	0	B
7	81	M	3:00	I	B
8	97	F	2:40	I	B
9	84	M	47:25	I	B
10	87	M	4:25	I	C
11	93	M	20:49	I	C
12	86	F	6:50	III	C
13	94	M	13:00	III	C
14	87	F	4:21	III	C
15	82	F	10:32	III	C
16	89	F	16:11	III	C
17	90	F	64:07	V	C
18	86	F	19:51	V	C
19	93	F	13:28	V	C
20	70	M	35:42	V	C
21	80	F	6:41	V	C

Abbreviations: PMT, postmortem time; NFT, neurofibrillary tangle; SP, senile plaque.
[a] NFTs and SPs were staged according to the neuropathology staging system of Braak and Braak (1991).

aging), a stage at which entorhinal cortex but not frontal cortex contains NFTs, the number of granular tau oligomers present significantly increased compared to that in the Braak-stage 0 samples ($P = 0.0173$). In samples staged at Braak stage III, a stage at which both limbic areas and entorhinal cortex contain NFTs, the number of granular tau oligomers present also significantly increased compare to that in the Braak-stage 0 samples ($P = 0.0087$). In samples staged at Braak stage V, a stage at which neocortex including frontal cortex contain NFTs, the number of granules increased again significantly compare to that in Braak-stage 0 samples ($P = 0.0087$). We observed no significant differences in the number of granular tau oligomers in stage I, III, and V samples.

We confirmed these results by using Western blotting to assess granular tau oligomer fractions and conventionally purified sarcosyl-insoluble tau fractions derived from Braak-staged frontal cortices (Fig. 2b and c, respectively). The Tau-c immunostaining intensity of tau bands derived from the granular tau oligomer fraction of Braak-stage 0 samples was faint (Fig. 2b). Nonetheless, in Braak-stage I, III, and V samples, we did detect tau smears displaying a immunostaining pattern characteristic of insoluble tau (Fig. 2b cf. PHF-1 immunostaining pattern in Fig. 2c) (Selkoe et al., 1982; Ihara et al., 1983; Greenberg and Davies, 1990). Linear regression analysis revealed a significant correlation between Tau-c immunoreactivity and the number of granular tau oligomers ($P < 0.0001$, $r^2 = 0.6336$). On the other hand, similar statistical analysis failed to reveal a correlation between PHF-1 immunoreactivity and the number of granular tau oligomers.

Taken together, these results indicate that granular tau oligomer levels begin to increase in pre-symptomatic stages of disease, suggesting that granular tau oligomers may form before NFTs are formed.

4. Discussion

4.1. Granular tau oligomer as a pre-symptomatic marker for AD

Using silver-stained human brain sections, Braak and Braak (1991) described seven stages (0–VI) of neuropathology that are now commonly used to stage the progression of neurodegenerative diseases. The Braak staging system is based on the density and distribution of agyrophilic NFTs in the brain (Braak and Braak, 1991). Stage 0 is characterized by the absence of NFTs. Stages I and II are termed transentorhinal stages, because they are characterized by the presence of NFTs in the transentorhinal region. Stages I and II are distinguished by the density of NFTs. Stages III and IV are termed limbic stages, because they are characterized by the presence of NFTs in the hippocampus as well as in the transentorhinal region. Stages V and VI are termed isocortical stages, because they are

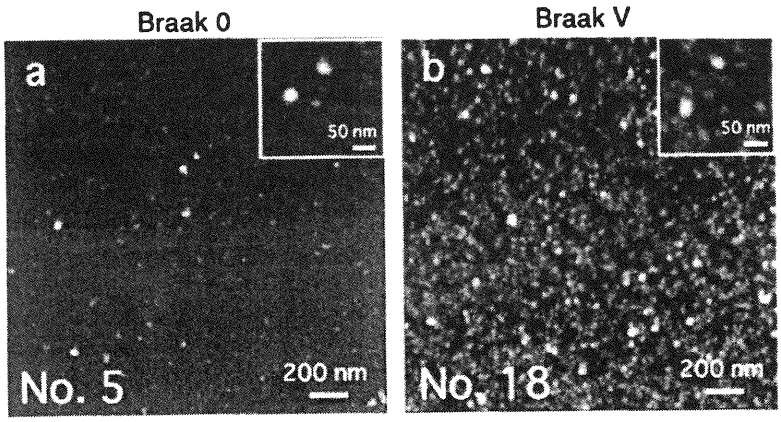

Fig. 1. Granular tau oligomers purified from human frontal cortex. Frontal cortex homogenates were fractionated with sucrose gradient centrifugation, and fractions (fraction 3) containing granular tau oligomers were examined in solution with AFM set to tapping mode. Representative data from the Braak-staged samples indicated are shown here. Insets contain high magnification AFM images of granular tau oligomers. The height range is 30 nm. The large numbers in the lower left corner of each panel correspond to the brain identification numbers in Table 1.

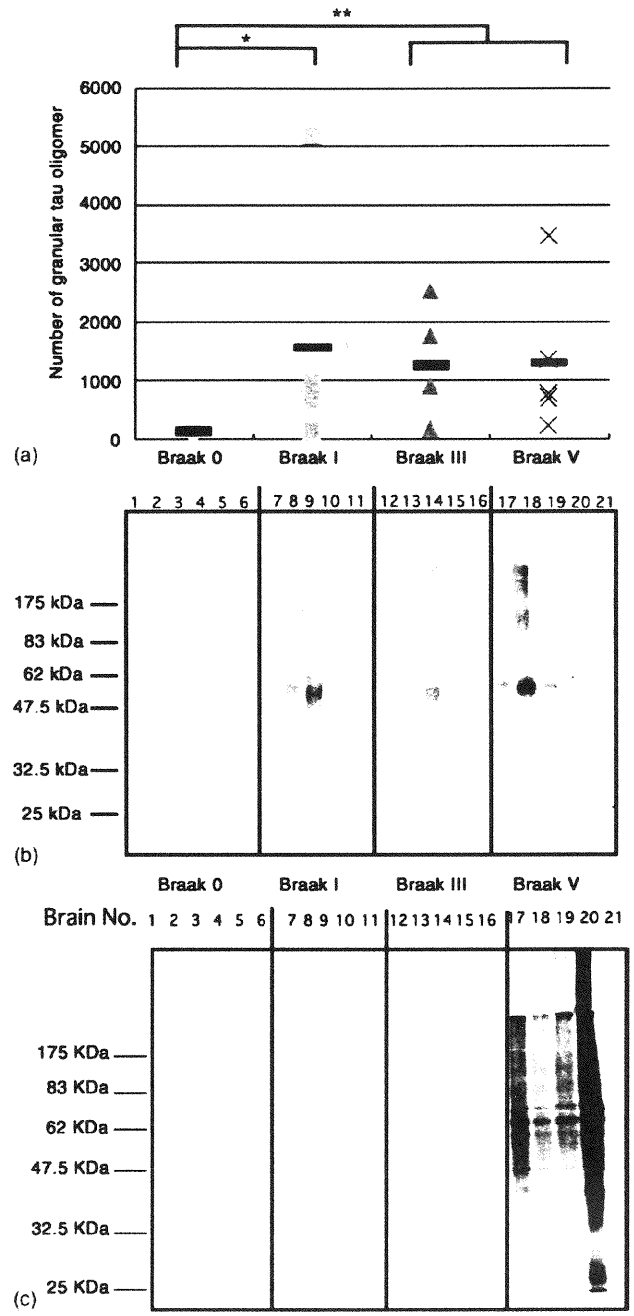

Fig. 2. The distribution of granular tau oligomers observed in different Braak stages. (a) AFM images of Braak-staged frontal cortex samples were analyzed with NIH-image 1.63, and the total number of granular aggregates in each sample were counted and graphed. $^{*}P < 0.05$, $^{**}P < 0.01$. (b) Western blots of fractions containing granular tau oligomers immunostained with Tau-c antibody. (c) Western blots of sarcosyl-insoluble fractions immunostained with PHF-1 antibody for the detection of tau filaments.

characterized by the extension of NFTs into neocortex, including frontal cortex.

The density and distribution of NFTs have been shown to increase with normal aging (Braak and Braak, 1997). Even non-AD brain specimens from individuals as old as 90 years contain NFTs. In Braak stage I, NFTs are confined within the transentorhinal region. Most of these NFTs are not accompanied by SPs, suggesting that that NFT formation occurring within the transentorhinal region is independent of SP formation, and thus may not represent a pathological process linked to AD. In line with these data is the finding that the anatomical distribution of NFTs observed in Braak stage I appears to be age dependent (Braak and Braak, 1997), which is consistent with the premise that NFT development occurs as part of normal brain aging.

We detected an increased amount of granular tau oligomers in Braak-stage I frontal cortex samples but not in Braak-stage 0 samples, suggesting that, at a time when NFTs form in the entorhinal cortex, tau dysfunction, which tau comes up from microtubule, and forms aggregate, has already started to occur in the frontal cortex, which should indicate tau dysfunction (Lu and Wood, 1993; Yoshida and Ihara, 1993). Interestingly, the level of granular tau oligomers in frontal cortex remained constant in samples staged at Braak stages II–V, even though the density of NFTs increases progressively in these stages. At this point, however, we cannot explain the incongruity between the levels of tau oligomers and NFTs. We do not know exactly how granular tau oligomers affect neuronal vulnerability.

We also investigated the relationship between granular tau oligomer formation and the density and distribution of senile plaques (SPs) (data not shown), another neuropathological hallmark of AD. We found granular tau oligomers in samples containing SPs in the neocortex (SP-stage B and C). In one Braak-stage 0 sample from an SP-stage B patient (No. 6 in Table 1), however, we did not detect a significant increase in granular tau oligomer levels, suggesting that the extent of SP pathology may not affect the formation of granular tau oligomers. Recently, Katsuno and colleagues reported that the accumulation of AB and tau occurs independently in entorhinal cortex (Katsuno et al., 2005). Therefore, the formation of granular tau oligomers may not be related to Aβ accumulation but instead may be related to some other aging-related event that occurs during Braak stage I. In later Braak stages, Aβ may accelerate the formation of granular tau oligomers that ultimately leads to NFT formation and neuronal loss. Further studies are required in order to understand the precise biochemical sequence of events underlying neuronal death, NFT formation, and granular tau oligomer formation.

References

Braak, H., Braak, E., 1991. Neuropathological stageing of Alzheimer-related changes. Acta Neuropathol. (Berl) 239–259.

Braak, H., Braak, E., 1997. Frequency of stages of Alzheimer-related lesions in different age categories. Neurobiol. Aging 351–357.

Gomez-Isla, T., Hollister, R., West, H., Mui, S., Growdon, J.H., Petersen, R.C., Parisi, J.E., Hyman, B.T., 1997. Neuronal loss correlates with but exceeds neurofibrillary tangles in Alzheimer's disease. Ann. Neurol. 17–24.

Greenberg, S.G., Davies, P., 1990. A preparation of Alzheimer paired helical filaments that displays distinct tau proteins by polyacrylamide gel electrophoresis. Proc. Natl. Acad. Sci. U.S.A. 5827–5831.

Hansma, H.G., Laney, D.E., Bezanilla, M., Sinsheimer, R.L., Hansma, P.K., 1995. Applications for atomic force microscopy of DNA. Biophys. J. 1672–1677.

Ihara, Y., 2001. PHF and PHF-like fibrils—cause or consequence? Neurobiol. Aging 123–126.

Ihara, Y., Abraham, C., Selkoe, D.J., 1983. Antibodies to paired helical filaments in Alzheimer's disease do not recognize normal brain proteins. Nature 727–730.

Jicha, G.A., O'Donnell, A., Weaver, C., Angeletti, R., Davies, P., 1999. Hierarchical phosphorylation of recombinant tau by the paired-helical filament-associated protein kinase is dependent on cyclic AMP-dependent protein kinase. J. Neurochem. 214–224.

Katsuno, T., Morishima-Kawashima, M., Saito, Y., Yamanouchi, H., Ishiura, S., Murayama, S., Ihara, Y., 2005. Independent accumulations of tau and amyloid beta-protein in the human entorhinal cortex. Neurology 687–692.

Lee, V.M., Goedert, M., Trojanowski, J.Q., 2001. Neurodegenerative tauopathies. Annu. Rev. Neurosci. 1121–1159.

Lu, Q., Wood, J.G., 1993. Functional studies of Alzheimer's disease tau protein. J. Neurosci. 508–515.

Murayama, S., Saito, Y., 2004. Neuropathological diagnostic criteria for Alzheimer's disease. Neuropathology 254–260.

Reed, L.A., Wszolek, Z.K., Hutton, M., 2001. Phenotypic correlations in FTDP-17. Neurobiol. Aging 89–107.

Saito, Y., Ruberu, N.N., Sawabe, M., Arai, T., Tanaka, N., Kakuta, Y., Yamanouchi, H., Murayama, S., 2004. Staging of argyrophilic grains: an age-associated tauopathy. J. Neuropathol. Exp. Neurol. 911–918.

Santacruz, K., Lewis, J., Spires, T., Paulson, J., Kotilinek, L., Ingelsson, M., Guimaraes, A., DeTure, M., Ramsden, M., McGowan, E., Forster, C., Yue, M., Orne, J., Janus, C., Mariash, A., Kuskowski, M., Hyman, B., Hutton, M., Ashe, K.H., 2005. Tau suppression in a neurodegenerative mouse model improves memory function. Science 476–481.

Selkoe, D.J., Ihara, Y., Salazar, F.J., 1982. Alzheimer's disease: insolubility of partially purified paired helical filaments in sodium dodecyl sulfate and urea. Science 1243–1245.

Takashima, A., Murayama, M., Murayama, O., Kohno, T., Honda, T., Yasutake, K., Nihonmatsu, N., Mercken, M., Yamaguchi, H., Sugihara, S., Wolozin, B., 1998. Presenilin 1 associates with glycogen synthase kinase-3beta and its substrate tau. Proc. Natl. Acad. Sci. U.S.A. 9637–9641.

Tanemura, K., Akagi, T., Murayama, M., Kikuchi, N., Murayama, O., Hashikawa, T., Yoshiike, Y., Park, J.M., Matsuda, K., Nakao, S., Sun, X., Sato, S., Yamaguchi, H., Takashima, A., 2001. Formation of filamentous tau aggregations in transgenic mice expressing V337M human tau. Neurobiol. Dis. 1036–1045.

Tanemura, K., Murayama, M., Akagi, T., Hashikawa, T., Tominaga, T., Ichikawa, M., Yamaguchi, H., Takashima, A., 2002. Neurodegeneration with tau accumulation in a transgenic mouse expressing V337M human tau. J. Neurosci. 133–141.

Tatebayashi, Y., Miyasaka, T., Chui, D.H., Akagi, T., Mishima, K., Iwasaki, K., Fujiwara, M., Tanemura, K., Murayama, M., Ishiguro, K., Planel, E., Sato, S., Hashikawa, T., Takashima, A., 2002. Tau filament formation and associative memory deficit in aged mice expressing mutant (R406W) human tau. Proc. Natl. Acad. Sci. U.S.A. 13896–13901.

von Bergen, M., Barghorn, S., Biernat, J., Mandelkow, E.M., Mandelkow, E., 2005. Tau aggregation is driven by a transition from random coil to beta sheet structure. Biochim. Biophys. Acta 158–166.

Wittmann, C.W., Wszolek, M.F., Shulman, J.M., Salvaterra, P.M., Lewis, J., Hutton, M., Feany, M.B., 2001. Tauopathy in *Drosophila*: neurodegeneration without neurofibrillary tangles. Science 711–714.

Yoshida, H., Ihara, Y., 1993. Tau in paired helical filaments is functionally distinct from fetal tau: assembly incompetence of paired helical filament-tau. J. Neurochem. 1183–1186.

Neuropathology and Applied Neurobiology (2006), **32**, 374–387 doi: 10.1111/j.1365-2990.2006.00736.x

Comparison of extent of tau pathology in patients with frontotemporal dementia with Parkinsonism linked to chromosome 17 (FTDP-17), frontotemporal lobar degeneration with Pick bodies and early onset Alzheimer's disease

A.-M. Shiarli[1], R. Jennings[1], J. Shi[1,2], K. Bailey[1], Y. Davidson[1], J. Tian[1,2], E. H. Bigio[3], B. Ghetti[4], J. R. Murrell[4], M. B. Delisle[5], S. Mirra[6], B. Crain[7], P. Zolo[8], K. Arima[9], E. Iseki[10], S. Murayama[11], H. Kretzschmar[12], M. Neumann[12], C. Lippa[13], G. Halliday[14], J. MacKenzie[15], N. Khan[16], R. Ravid[17], D. Dickson[18], Z. Wszolek[18], T. Iwatsubo[19], S. M. Pickering-Brown[1,18] and D. M. A. Mann[1]

[1]Clinical Neuroscience Research Group, University of Manchester, Greater Manchester Neurosciences Centre, Hope Hospital, Salford, UK. [2]Department of Care of the Elderly, Dongzhimen Hospital, Beijing University of Chinese Medicine, Beijing, China. [3]North western University Alzheimer's Disease Center, Chicago, IL, USA, [4]Indiana Alzheimer Disease Centre, Indiana University School of Medicine, Indianapolis, IN, USA, [5]Service d'Anatomie et de Cytologie Pathologiques, Hopitaux de Toulouse, Toulouse, Cedex 4, France, [6]Department of Pathology, State University of New York Health Science Center at Brooklyn, Brooklyn, NY, USA, [7]Department of Pathology, Johns Hopkins University School of Medicine, Baltimore, MD, USA, [8]San Donato Medical Center, Arezzo, Italy, [9]National Centre Hospital for Mental, Nervous and Muscular Disorders, Tokyo, Japan. [10]Juntendo Tokyo Koto Geriatric Medical Center, Juntendo University School of Medicine, Tokyo, Japan, [11]Department of Neuropathology, Tokyo Metropolitan Institute of Gerontology, Tokyo, Japan. [12]Reference Centre for Prion Diseases and Neurodegenerative Diseases, Institute of Neuropathology, Marchioninistr 17, Munchen, Germany, [13]Memory Disorders Centre, Drexel University College of Medicine, Philadelphia, PA, USA, [14]Department of Neuropathology, Prince of Wales Medical Research Institute, University of New South Wales, Randwick, NSW, Australia, [15]The Royal Infirmary, Foresterhill, Aberdeen, Scotland, [16]The Brain Bank, Institute of Psychiatry, London, UK, [17]Netherlands Brain Bank, Meibergdreef 33, Amsterdam, the Netherlands, [18]Mayo Clinic, 4500 San Pablo Road, Jacksonville, FL, USA, [19]Department of Neuropathology and Neuroscience, University of Tokyo, Tokyo, Japan

---

A.-M. Shiarli, R. Jennings, J. Shi, K. Bailey, Y. Davidson, J. Tian, E. H. Bigio, B. Ghetti, J. R. Murrell, M. B. Delisle, S. Mirra, B. Crain, P. Zolo, K. Arima, E. Iseki, S. Murayama, H. Kretzschmar, M. Neumann, C. Lippa, G. Halliday, J. MacKenzie, N. Khan, R. Ravid, D. Dickson, Z. Wszolek, T. Iwatsubo, S. M. Pickering-Brown and D. M. A. Mann (2006) *Neuropathology and Applied Neurobiology* **32**, 374–387

Comparison of extent of tau pathology in patients with frontotemporal dementia with Parkinsonism linked to chromosome 17 (FTDP-17), frontotemporal lobar degeneration with Pick bodies and early onset Alzheimer's disease

In order to gain insight into the pathogenesis of frontotemporal lobar degeneration (FTLD), the mean tau load in frontal cortex was compared in 34 patients with frontotemporal dementia linked to chromosome 17 (FTDP-17) with 12 different mutations in the *tau* gene (*MAPT*), 11 patients with sporadic FTLD with Pick bodies and 25 patients with early onset Alzheimer's disease (EOAD). Tau load was determined, as percentage of tissue occupied by stained product, by image analysis of immunohistochemically stained sections using the phospho-dependent antibodies AT8, AT100 and AT180. With AT8 and AT180 antibodies, the amount of tau was significantly ($P < 0.001$

Correspondence: David M. A. Mann, Clinical Neuroscience Research Group, University of Manchester, Greater Manchester Neurosciences Centre, Hope Hospital, Salford, M6 8HD, UK. Tel: +44 0161 206 2580; Fax: +44 0161 206 0388; E-mail: david.mann@manchester.ac.uk

in each instance) less than that in EOAD for both FTDP-17 (8.5% and 10.0% respectively) and sporadic FTLD with Pick bodies (16.1% and 10.0% respectively). With AT100, the amount of tau detected in FTDP-17 was 54% ($P < 0.001$) of that detected in EOAD, but no tau was detected in sporadic FTLD with Pick bodies using this particular antibody. The amount of insoluble tau deposited within the brain in FTDP-17 did not depend in any systematic way upon where the *MAPT* mutation was topographically located within the gene, or on the physiological or structural change generated by the mutation, regardless of which anti-tau antibody was used. Not only does the amount of tau deposited in the brain differ between the three disorders, but the pattern of phosphorylation of tau also varies according to disease. These findings raise important questions relating to the role of aggregated tau in neurodegeneration – whether this represents an adaptive response which promotes the survival of neurones, or whether it is a detrimental change that directly, or indirectly, brings about the demize of the affected cell.

Keywords: Tau protein, Tau gene, Alzheimer's disease, frontotemporal lobar degeneration, neurofibrillary tangle, Pick bodies

Introduction

Frontotemporal lobar degeneration (FTLD) is a descriptive term given to a clinically and pathologically heterogeneous group of early onset, non-Alzheimer forms of dementia. A previous family history of a similar disorder occurs in about half of patients, and a consensus conference in 1997 highlighted the observations that many such families were linked to a locus on chromosome 17, following which the term frontotemporal dementia with Parkinsonism linked to chromosome 17 (FTDP-17) was derived [1]. In 1998, the disorder was shown [2–4], in certain of these chromosome 17-linked families, to be associated with mutational events in the *tau* gene (*MAPT*), located on the long arm of chromosome 17 (17q21–22). The prevalence of *MAPT* mutations within patients with FTLD varies from about 6–18% [5–7].

To date, more than 35 *MAPT* mutations in over 150 families have been identified, and there is much clinical as well as pathological heterogeneity among the various mutations (see [8,9] for reviews). Some *MAPT* mutations exist as missense mutations within coding regions of exons 1, 9, 11, 12 and 13 [2,3,6,10–19]. Generally, cases with these mutations show swollen nerve cells, and rounded intraneuronal inclusions, reminiscent of the Pick bodies typically seen in some cases of sporadic FTLD, mainly within large and small pyramidal neurones of the cerebral cortex and pyramidal and granule cells of the hippocampus [10–19]. These mutations affect all six isoforms of tau and generate mutated tau molecules that (variably) lose their ability to interact with microtubules, thereby interfering with the promotion of microtubule assembly and axonal transport [2,3,6,10–20]. Some of the mutations also increase, but again variably, the propensity of the mutated tau to self-aggregate into fibrils that form the characterizing pathological structures within the brain [14–16,18–20].

Other *MAPT* mutations lie close to the splice donor site of the intron that follows the alternatively spliced exon 10 [2–4,6,20–35]. Such cases typically show insoluble aggregated tau deposits as neurofibrillary tangle (NFT)-like structures within large and smaller pyramidal cells of cortical layers III and V, and prominently within glial cells in the deep white matter, globus pallidus and internal capsule [23,27,30–34,36,37]. This group of mutations cluster around, or lie within a predicted regulatory stem loop structure of a splice acceptor domain of *MAPT* that determines the inclusion or exclusion of exon 10 by alternative splicing during gene transcription. Such mutations may destabilize this stem loop, and disrupt its function, interfering with the binding of U1snRNP splice regulatory elements, increasing the proportion of tau mRNA transcripts containing exon 10, and the amount of 4-repeat (4R) tau, relative to 3-repeat (3R) tau, protein [2,3]. Other mutations within exon 10 interfere with the splicing ratio between 3R and 4R tau either by strengthening [22,26,35] or destroying [26] the function of splicing-enhancing elements, or by disrupting the function of a splice-silencing element [26,31], in the 5′ region of exon 10. Exon 10 mutations like P301L do not affect the splicing of exon 10 [2,26] but induce conformational changes in tau molecules containing exon 10 that interfere with microtubule function, and lead to a specific aggregation of the mutant 4R tau into fibrils [31,35].

Surveys of the published literature infer that not only the distribution and morphology of the insoluble tau aggregate vary greatly in patients with FTLD with *MAPT* mutations according to mutation site and type, but also the total amount of deposited tau can differ. Microscopic observation of cases of FTDP-17 with those of younger individuals with early onset Alzheimer's disease (EOAD) suggests a lower burden of tau pathology. Such observations are somewhat curious and paradoxical given the prevailing view that *MAPT* mutations are the root cause of clinical disability in FTDP-17, whereas in Alzheimer's disease (AD) tau pathology is considered to be a more downstream (to amyloid pathology) event. They also challenge the hypothesis that the accumulation of tau within nerve cells is detrimental to the health of the cell and responsible for its demize.

In the present study we have therefore measured, by image analysis of tau-immunostained sections, and compared the amount of insoluble tau proteins (tau load) in the brains of patients with FTDP-17 with 12 different *MAPT* mutations, patients with sporadic FTLD with Pick bodies and other patients with EOAD.

Materials and methods

Brain tissues were available at autopsy from 34 cases of FTDP-17 with 12 different *MAPT* mutations. Six cases (cases #19–24), one with *MAPT* exon 10 +13 mutation (case #19), and five with *MAPT* exon 10 +16 mutation (cases #20–24) were obtained from the Manchester Brain Bank [37], whereas tissue samples from the other 28 FTDP-17 cases were kindly supplied in collaboration by colleagues from different centres across the world. Selected clinical and pathological details for all cases are given in Table 1. Full clinical and pathological descriptions for 31 of the 34 cases of FTDP-17 have been previously reported by the originating authors (see Table 1 for details of citation); the other three cases remain unreported to date. The 34 FTDP-17 cases (18 men and 16 women) (see Table 1) had mean age of onset of disease of 48.5 ± 7.8 years, range 32–65 years with mean age of death was 57.3 ± 10.0 years, range 38–78 years. The mean disease duration was 8.5 ± 5.5 years, range 2–27. Twelve cases had *APOE* ε3/ε3 genotype, seven had ε3/ε4 genotype, five had ε2/ε3 genotype and one was ε2/ε2. Only in cases #19 and 20 were there any additional AD-type changes, and then only in the form of some diffuse amyloid plaques. Neither case had sufficient AD-type pathology to warrant (additional) diagnosis of AD under Consortium to Establish a Registry for Alzheimer's Disease (CERAD) criteria [38]. Braak staging (for AD) [39] was inappropriate.

Tissues were also obtained from 11 cases of sporadic FTLD (cases #35–45) from the Manchester Brain Bank collection, in whom previous pathological investigations [37 and unpublished Mann *et al.*] had shown Pick bodies to be present in the cerebral cortex and hippocampus. Pick bodies were identified, as defined by Kertesz *et al.* [40], as round or oval, compact intracytoplasmic neuronal inclusions, stained by Bielschowsky but not by Gallyas, tau-immunoreactive and located in dentate fascia, hippocampus and cerebral cortex. The 11 cases (six men and five women) had a mean age of onset of disease of 57.6 ± 10.4 years, range 46–76 years and mean age of death 66.5 ± 9.2 years, range 56–84 years. The mean disease duration was 8.9 ± 2.7 years, range 4–14 years. Five patients had *APOE* ε3/ε3 genotype, two had ε3/ε4 genotype, two had ε2/ε3 genotype and one was ε2/ε2. None of these cases showed any coincidental AD-type pathology.

All 25 cases of EOAD (11 men and 14 women) were from the Manchester Brain Bank collection. These had a mean age of onset of disease of 53.4 ± 6.6 years, range 35–60 years and mean age of death 62.9 ± 8.0 years, range 44–73 years. The mean disease duration was 9.5 ± 3.5 years, range 4–19 years. Sixteen patients had *APOE* ε3/ε3 genotype, seven had ε3/ε4 genotype, one had ε2/ε3 genotype and one had ε2/ε2 genotype. All cases were consistent with CERAD pathological criteria for AD [38], and all were at Braak stages 5 or 6 [39]. In none of the cases was there a previous family history of disease consistent with autosomal dominant inheritance.

We chose not to include a control group of nondemented persons within the study because the primary purpose was to investigate how the level of tau deposition in FTLD compared with that in EOAD. Moreover, the great majority of cases studied, FTLD or AD, were less than 65 years of age at death, and it is uncommon for significant tau pathology to be present in normal individuals in that age range. Furthermore, although cases of corticobasal degeneration (CBD) and progressive supranuclear palsy (PSP) are subsumed under some pathological criteria for FTLD [41], we did not include such cases in this present study. This was because in CBD, tau pathology is within glial cells as well as neurones, and principally affects parietal cortex rather than frontal lobes, whereas

Table 1. Selected clinical and pathological details of cases investigated

Case	*Diagnosis*	MAPT *mutation*	*Gender*	*Age at onset (year)*	*Age at death (year)*	*Duration (year)*	APOE *genotype*	*Brain weight (g)*
1 [18]	FTDP-17	L266V	M	32	36	3.5	NA	1050
2 [30]	FTDP-17	N279K	M	46	57	11	3,3	1250
3 [30]	FTDP-17	N279K	M	44	50	6	3,3	1420
4 [20]	FTDP-17	N279K	M	44	50	6	3,4	1290
5 [20]	FTDP-17	N279K	F	45	48	3	3,3	1100
6 [20]	FTDP-17	N279K	M	56	58	2	2,3	1400
7 [20]	FTDP-17	N279K	F	45	53	8	2,4	1000
8 [20]	FTDP-17	N279K	M	57	63	6	3,4	1100
9 [20]	FTDP-17	N279K	M	41	52	11	2,3	1100
10 [25]	FTDP-17	N279K	M	40	47	7	NA	1230
11 [33]	FTDP-17	N296H	M	57	62	3	3,3	960
12 [6,21]	FTDP-17	P301L	M	48	60	12	3,3	1331
13 [6,21]	FTDP-17	P301L	F	50	66	15	3,3	856
14 [6,21]	FTDP-17	P301L	M	44	52	8	2,3	1087
15 [6,21]	FTDP-17	P301L	F	54	76	22	2,2	1006
16 [6,21]	FTDP-17	P301L	F	59	64	5	3,3	1013
17 [28]	FTDP-17	P301L	F	48	55	7	NA	915
18 [32,36]	FTDP-17	S305S	F	48	51	3	NA	1053
19 [2,34]	FTDP-17	Exon 10 +13	M	65	70	5	3,4	1100
20 [2,34]	FTDP-17	Exon 10 +16	M	50	61	11	3,4	1016
21 [2,34]	FTDP-17	Exon 10 +16	F	46	58	12	3,3	996
22 [2,34]	FTDP-17	Exon 10 +16	M	43	55	12	3,4	1240
23 [34]	FTDP-17	Exon 10 +16	F	52	65	13	2,3	1040
24 [34]	FTDP-17	Exon 10 +16	F	48	56	8	3,4	1175
25 [un]	FTDP-17	Exon 10 +16	F	43	52	9	2,3	1138
26 [19]	FTDP-17	Q336R	M	58	68	10	3,3	1102
27 [12]	FTDP-17	G342V	F	48	55	7	3,3	1020
28 [15]	FTDP-17	K369I	F	52	61	9	NA	885
29 [13]	FTDP-17	G389R	F	32	37	5	3,3	1006
30 [un]	FTDP-17	G389R	M	45	49	4	NA	1170
31 [11]	FTDP-17	G389R	M	38	43	5	NA	NA
32 [6,21]	FTDP-17	R406W	M	63	70	7	3,3	1121
33 [6,21]	FTDP-17	R406W	F	58	71	13	3,4	905
34 [un]	FTDP-17	R406W	F	49	78	29	NA	1035
35 [37]	Pick	None	F	53	60	7	3,3	960
36 [37]	Pick	None	M	46	56	10	3,3	1150
37 [37]	Pick	None	M	NA	NA	NA	NA	NA
38 [37]	Pick	None	F	52	62	10	3,4	928
39 [37]	Pick	None	F	76	84	8	3,3	1235
40 [37]	Pick	None	F	50	58	8	2,2	1065
41 [37]	Pick	None	M	63	74	11	2,3	990
42 [37]	Pick	None	M	73	77	4	3,3	NA
43 [37]	Pick	None	F	57	64	7	3,3	1000
44 [37]	Pick	None	M	47	61	14	3,4	980
45 [un]	Pick	None	M	59	69	10	2,3	NA
46	AD	None	F	54	59	5	3,3	1008
47	AD	None	F	56	62	6	3,3	1020
48	AD	None	M	55	60	5	3,4	1368
49	AD	None	F	57	67	10	3,4	1018
50	AD	None	F	39	45	6	3,3	NA
51	AD	None	M	40	44	4	3,3	1400
52	AD	None	F	52	71	19	3,3	910
53	AD	None	M	35	45	10	3,4	1177

Table 1. *Continued*

Case	*Diagnosis*	MAPT *mutation*	*Gender*	*Age at onset (year)*	*Age at death (year)*	*Duration (year)*	APOE *genotype*	*Brain weight (g)*
55	AD	None	F	58	70	12	3,4	1026
56	AD	None	F	52	61	9	3,3	906
57	AD	None	F	52	64	12	2,2	1120
58	AD	None	F	54	67	13	3,3	947
59	AD	None	M	55	61	6	3,3	NA
60	AD	None	M	60	72	12	3,4	1251
61	AD	None	F	60	73	13	3,3	1028
62	AD	None	F	52	61	9	3,3	1262
63	AD	None	M	56	66	10	3,3	1070
64	AD	None	F	59	71	12	3,3	1208
65	AD	None	M	55	64	9	2,3	1275
66	AD	None	F	48	60	12	3,4	1050
67	AD	None	M	59	64	5	3,3	1330
68	AD	None	M	57	67	10	3,3	1158
69	AD	None	M	60	66	6	3,3	1206
70	AD	None	M	58	70	12	3,4	1314

FTDP-17, frontotemporal dementia with Parkinsonism linked to chromosome 17; Pick, frontotemporal lobar degeneration with Pick bodies; AD, Alzheimer's disease; un, unpublished case. NA, no details available. Citation numbers in parentheses.

in PSP, tau pathology is mostly within neurones and glial cells in subcortical structures. Therefore, although such disorders can likewise be considered as tauopathies, measurement of tau load within frontal cortex was not considered to be informative, at least as regards the purpose of the present investigation.

Serial sections from formalin-fixed, wax-embedded blocks of frontal cortex (BA 8/9) were cut at a thickness of 6 μm and mounted on 3-aminopropyltrieihoxysilane (APES)-coated slides. Sections were immunostained for insoluble tau proteins by a standard immunoperoxidase method [37], using the phospho-dependent tau antibodies AT8 (1 : 750 dilution), AT100 (1 : 200 dilution) and AT180 (1 : 200 dilution) (all from Innogenetics, Belgium). AT8 antibody is raised against phosphorylated Ser202 epitope and immunoreacts with paired helical filament (PHF) tau in AD [42]. AT100 antibody is raised against phosphorylated Thr212/Ser214 epitopes and labels only pathological tau [43]. AT180 antibody is raised against phosphorylated Thr231 epitope, and labels approximately 70% of PHF in AD brain, but also labels phosphorylated foetal and adult normal tau [44].

The amount of insoluble tau (tau load) within AT8-, AT100- and AT180-immunostained sections was quantified by Image Analysis. The system employed uses Leica Image Analysis software and a Leica Microscope with Quantimet 570 Image Analyser. Measurement of tau load was performed only on grey matter regions. The area for measurement, which extended from the surface of the cortex to the grey/white matter boundary, was identified under the microscope at ×5 magnification. After optimizing the computer captured image for colour and staining density, the total measured area and area of tissue occupied by stained product were determined using in-house software. The software employed allows the segmented image to be directly overlaid upon the captured image so that with optimal thresholding it can be ensured that all tau-immunostained stained objects (for example, NFT, neuropil threads and plaque neurites in AD, NFT or Pick bodies in FTLD and FTDP-17) are recognized. To ensure comparability between cases, the particular area measured was systematically sampled so that the measured field was always on a 'straight' section of the cortex, away from the depths or the crown of the gyrus, and away from 'bad quality tissue' (that is, tissue areas containing artefactual staining or splits or tears in the section). The total area of cortex measured in each field averaged 1.43 mm^2. Tau load was calculated as the percentage of total area occupied by immunostained product. Trial measurements, employing cumulative mean statistic, were initially performed to determine the number of fields required to be measured for the mean to fall within 95% confidence levels for each antibody. In this way it was determined that for AT8-immunostained sections six measurements were

necessary, and for AT100- and AT180-immunostained sections four measurements were required. The mean tau load was calculated for each section.

Image Analysis data was analysed using the Statsdirect statistical package. Because the mean tau load data obtained from AT8-immunostained sections did not follow a normal distribution, logarithmic transformation was performed. A one way analysis of variance test (ANOVA) was then used to compare differences in tau deposition between each disease group with *post hoc* unpaired *t*-tests being performed where results of ANOVA were significant. The tau load data obtained for sections stained with AT100 and AT180 likewise did not follow a normal distribution, even when logarithmically transformed. Therefore, Kruskal–Wallis test was used to compare differences in tau deposition between each disease group with *post hoc* Mann–Whitney *U*-tests being performed when result of Kruskal–Wallis was significant. Comparison of tau load between bearers and non-bearers of *APOE* ε4 allele in each disease group were performed for all antibodies using Mann–Whitney *U*-test. For all statistical tests a *P*-value less than 0.05 was considered significant.

In order to investigate the effect of different *MAPT* mutations on tau load, the cases were categorized into four groups according to mutation type:

Group A – cases ($n = 18$) with *MAPT* mutations which affect splicing of exon 10 increasing the 4R : 3R ratio of tau isoforms and producing mostly NFT pathology (mutations: N279K, N296H, S305S, +16, +13).

Group B – cases ($n = 16$) with *MAPT* mutations which alter the tau protein and have been shown to affect microtubule binding (mutations: L266V, Q336R, G342V, K369I, G389R, P301L, R406W).

Group C – cases ($n = 7$) with *MAPT* mutations which alter the tau protein and have been shown to affect microtubule binding, but produce only Pick-type pathology (mutations: L266V, Q336R, G342V, K369I, G389R).

Group D – cases ($n = 9$) with *MAPT* mutations which alter the microtubule binding of the protein, but do not affect exon 10 splicing, and produce mostly NFT-type pathology (mutations: P301L, R406W)

Mann–Whitney *U*-tests were performed between these groups to investigate differences in tau deposition between different groups of *MAPT* mutations. Mann–Whitney *U*-test was also performed to investigate differences in tau deposition between FTDP-17 group C cases with Pick-type bodies and sporadic FTLD cases with Pick bodies. Mann–Whitney *U*-tests were also performed to assess differences in relative immunoreactivity between AT8, AT100 and AT180 antibodies, for each disease group. Spearman rank correlation test was used to determine correlations between tau load and duration and age of onset of disease in each disease group.

Results

Morphological descriptions of tau pathology, using the present, or other similar, tau antibodies, on those FTDP-17 patients studied here have been fully reported previously by both ourselves [13,19,34,37] and other workers [6,10–12,15,18,25,28,30,32–34,36], as have those patients with sporadic FTLD with Pick bodies from our own series of FTLD cases [37], and such observations are therefore not repeated in this present study. Likewise, the immunohistochemical pattern of tau pathology in the AD cases was entirely typical of the disorder, and is likewise not described further in this report.

Comparison of tau load between the three disease groups

Mean tau load detected for each disease group, for each antibody, is shown in Table 2. For AT8 antibody, there was a highly significant difference in tau load between the three disease groups ($F_{2,67} = 44.4$; $P < 0.0001$) so that mean tau load in FTDP-17, and in sporadic FTLD with Pick bodies, were both significantly less ($P < 0.001$) than that in EOAD. There was a trend ($P = 0.057$) towards

Table 2. Mean (± SD) tau load in frontal cortex as detected by phospho-dependent antibodies AT8, AT100 and AT180 in 34 patients with FTDP-17, 11 with sporadic FTLD with Pick bodies and 25 with EOAD

	AT8	*AT100*	*AT180*
FTDP-17	1.2 ± 1.1	1.5 ± 1.5	0.9 ± 0.8
MAPT mutation Group A	1.1 ± 1.2	1.1 ± 1.5	0.7 ± 0.9
MAPT mutation Group B	1.4 ± 1.0	2.0 ± 1.4	1.0 ± 0.6
MAPT mutation Group C	1.7 ± 1.2	1.6 ± 1.5	0.8 ± 0.5
MAPT mutation Group D	1.1 ± 0.8	2.2 ± 1.3	1.2 ± 0.7
Sporadic FTLD with Pick bodies	2.3 ± 1.5	0 ± 0	0.9 ± 0.6
EOAD	14.3 ± 12.8	2.8 ± 3.1	9.0 ± 11.0

FTDP-17, frontotemporal dementia with Parkinsonism linked to chromosome 17; FTLD, frontotemporal lobar degeneration; EOAD, early onset Alzheimer's disease.

mean tau load in FTDP-17 being less than that in sporadic FTLD with Pick bodies.

For AT180 antibody, using Kruskal–Wallis test, there was a highly significant difference in mean tau load between the three disease groups ($\chi^2 = 27.9$; $P < 0.0001$) so that mean tau load in FTDP-17, and in sporadic FTLD with Pick bodies, was significantly less ($P < 0.001$) than that in EOAD. There was no significant difference ($P = 0.918$) in mean tau load between FTDP-17 and sporadic FTLD with Pick bodies.

For AT100 antibody (again using Kruskal–Wallis test) there was also a highly significant difference in mean tau load between the three disease groups ($\chi^2 = 24.5$; $P < 0.0001$). Indeed, there was little or no (measurable) staining of Pick bodies with AT100. Mean tau load in FTDP-17, and in EOAD, was consequently greater ($P < 0.001$) than that in sporadic FTLD with Pick bodies. Mean tau load in FTDP-17 was less (but not significantly so, $P = 0.083$) than that in patients with EOAD.

Differences in tau deposition within the FTDP-17 group

The extent of tau deposition was compared in FTDP-17 according to *MAPT* mutation position or type. When plotted against the topographical position of the *MAPT* mutation (coding for the longest tau isoform), no clear cut individual differential effect of any of the *MAPT* mutations on the extent of tau deposition within the frontal cortex was seen, either for AT8, AT100 or AT180 antibodies (Figure 1). Nonetheless, with AT8 immunostaining, *MAPT* L266V and exon 10 +13 splice mutation showed

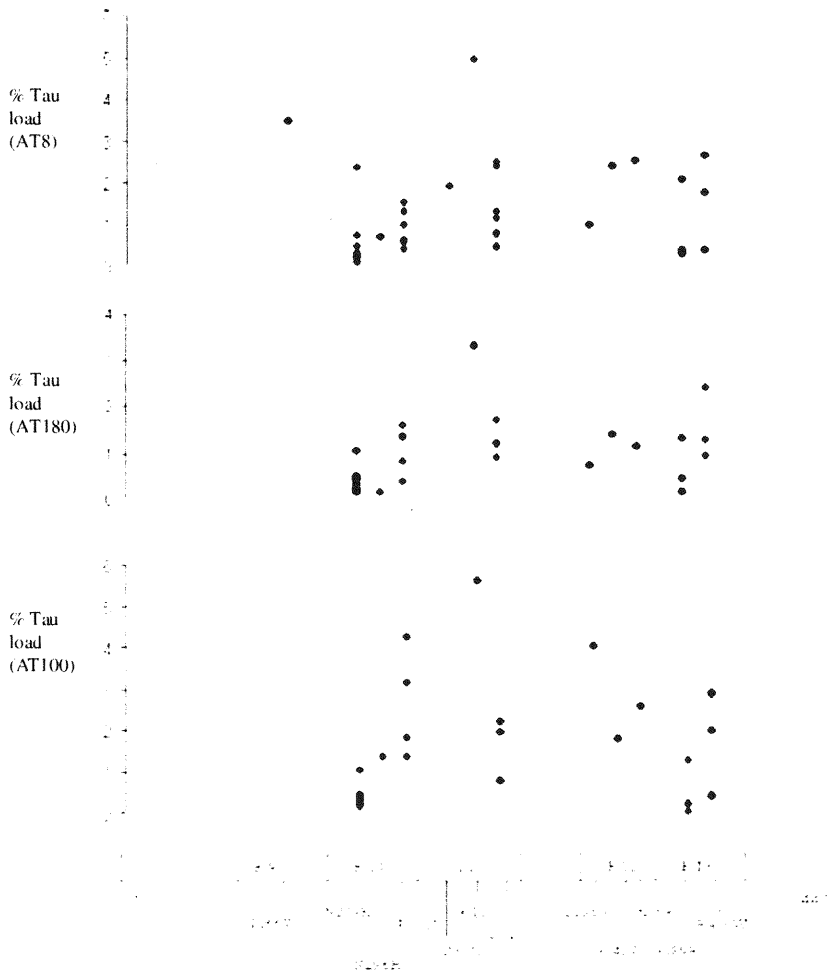

Figure 1. Tau load detected in each case for each of the mutations: E indicates exons on the gene; I indicates intron.

particularly heavy tau deposition, relative to the other cases. For L266V, this is consistent with the involvement of all the cortical layers of grey matter and some astrocytic staining in the pathological process (see also [18]). In the exon 10 +13 mutation, this could be explained by the presence of many tau-positive neuritic plaques in the superficial layers of the cortex (see also [34]). For AT180, again as explained, exon 10 +13 splice mutation showed particularly heavy tau deposition. However, for AT100 some of P301L cases, and the Q336R case, were heavily stained relative to AT8 and AT100 (Figure 1).

As detailed in *Methods* section, the mutation cases were grouped in order to investigate the effect of different *MAPT* mutation types on tau load. No significant differences in mean tau load were seen between any of the four *MAPT* mutation groups as detected by either AT8 ($\chi^2 = 1.05$; $P = 0.789$), AT180 ($\chi^2 = 2.86$; $P = 0.413$) or AT100 ($\chi^2 = 6.52$; $P = 0.09$) antibodies (Table 2). The mean tau load in FTDP-17 cases with Pick-type bodies (that is, Group C cases) did not differ from that seen in sporadic FTLD with Pick bodies for either AT8 ($P = 0.375$) or AT180 antibodies ($P = 0.887$) (Table 2), although interestingly AT100 immunostained Pick bodies in Group C cases (cf lack of Pick body staining in sporadic FTLD with Pick bodies).

Comparisons of relative immunoreactivities of each antibody

In general, in FTDP-17, AT8 and AT100 gave similar degree of immunostaining, whereas AT180 antibody showed less immunoreactivity (Table 2), although for some *MAPT* mutations (for example, R406W, N279K, exon 10 +16, G389R mutations) the tau load detected by AT8 and AT180 antibodies was similar. Again, in general, AT100 antibody showed slightly more immunoreactivity than AT8, but in some instances AT8 and AT100 immunoreactivity was the same (for example, K369I, G342V, exon 10 +13 mutations) and for some (for example, P301L mutation) AT100 gave stronger staining than AT8. However, statistically, the mean tau load detected by AT8, AT100 or AT180 antibodies did not vary significantly ($\chi^2 = 2.1$; $P = 0.340$) (Table 2).

In sporadic FTLD with Pick bodies, and EOAD, mean tau load detected by each antibody varied significantly ($\chi^2 = 24.8$ and $\chi^2 = 22.4$ respectively; $P < 0.0001$ for both). *Post hoc* testing showed that in both of these disease groups, mean tau load detected by AT8 was greater than that detected by either AT100 ($P < 0.0001$ in both instances) or AT180 ($P = 0.004$ and $P = 0.026$ respectively), and that mean tau load detected by AT180 was greater than that detected by AT100 in both disease groups ($P < 0.0001$ in both instances).

Effect of possession of the *APOE* ε4 allele

Mean percentage tau load, as detected by AT8, AT100 or AT180 antibodies, in patients with *APOE* ε4 allele was not significantly different from that detected in those without *APOE* ε4 allele for any of the three disorders (Table 3)

Correlations with age of onset of disease and duration of illness

With AT8, no significant correlation between duration of illness and tau load was found for any of the three disorders ($r_s = 0.07$–0.09; $P = 0.595$–0.838). For the age of onset of disease no significant correlations were found

Table 3. Mean (±SD) tau load in frontal cortex as detected by phospho-dependent antibodies AT8, AT100 and AT180 in 34 patients with FTDP-17, 11 with sporadic FTLD with Pick bodies and 25 with EOAD, stratified into those bearing *APOE* ε4 allele and those without *APOE* ε4 allele

	APOE status	*AT8*	*AT100*	*AT180*
FTDP-17	With ε4 allele	1.7 ± 1.7	1.5 ± 1.6	1.2 ± 1.3
	Without ε4 allele	0.9 ± 0.7	1.9 ± 2.1	0.8 ± 0.6
Sporadic FTLD with Pick bodies	With ε4 allele	2.3 ± 1.5	0 ± 0	0.7 ± 0.8
	Without ε4 allele	2.3 ± 0.3	0 ± 0	1.0 ± 0.7
EOAD	With ε4 allele	15.0 ± 12.5	2.9 ± 3.3	12.5 ± 13.0
	Without ε4 allele	13.5 ± 12.5	2.8 ± 3.2	7.6 ± 10.3

FTDP-17, frontotemporal dementia with Parkinsonism linked to chromosome 17; FTLD, frontotemporal lobar degeneration; EOAD, early onset Alzheimer's disease.

with tau load for either FTDP-17 ($r_s = 0.09$; $P = 0.623$) or EOAD ($r_s = 0.37$; $P = 0.070$), but a significant inverse correlation was found in sporadic FTLD with Pick bodies ($r_s = -0.850$; $P = 0.002$). Similar findings were seen with AT100 and AT180 (data not shown).

Discussion

The effect of 12 different mutations in *MAPT* on the amount of tau protein deposited in the brain has been investigated in this study using immunohistochemical staining with three phosphorylation-dependent anti-tau antibodies. We grouped the mutations according to their functional effects, or pathological characteristics, looking for differences in effect between those mutations (Group A) which affect splicing of exon 10 increasing the 4R : 3R ratio of tau isoforms and produce mostly NFT pathology with those missense mutations outside exon 10 (Group B) that change the protein structure of tau and affect all tau isoforms and interfere with microtubule binding. We also compared mutations that generate a Pick body-like pathology (Group C) with those that alter the microtubule-binding capability of tau, but do not affect exon 10 splicing and produce mostly NFT-type pathology (Group D). In no instance did we find any significant group differences in the extent of tau deposition with any of the antibodies, nor did any single mutation appear to have any preferential effect in this respect, although singleton cases of L266V and exon 10 +13 splice mutation did show relative (to other mutations) high tau loads with AT8 and AT180. In the former case there were unusually high levels of tau within grey matter astrocytes [see, also 18], while in the latter case there was a heavy tau burden within neuritic plaques [see 34], in accordance with age and possession of *APOE* ε4 allele [45]. Some P301L cases and the single Q336R case showed disproportionately (relative to AT8 and AT180) high tau loads with AT100. Hence, we find that the amount of tau deposited in the brain in FTDP-17 does not seem to be determined either by topographic position within *MAPT*, or the physiological change in tau function induced by such a mutation. Neither does the isoform composition of the aggregated tau seem to influence the amount of tau deposited because there was no difference in tau load between Group B cases, which lead to a tau deposition with a mix of (mostly) 3R and 4R tau isoforms [see 10–13,15,18,19], and Group A cases, where the tau protein is known to be mostly, or only, 4R [see 22,25,28,30–34,36]. This implies that both types of mutation, despite having a different primary effect on the tau protein itself, ultimately affect cellular function (possibly microtubule stability) in a similar way and/or to a similar degree. Similarly, the amount of tau deposited in the form of Pick bodies in FTDP-17 is not different from that seen in cases of sporadic FTLD characterized by Pick body formation.

Interestingly, and perhaps paradoxically, the amount of tau deposited in FTDP-17 or in FTLD with Pick bodies, irrespective of the physiological change in tau invoked (that is, mutational or posttranslational respectively), as detected by AT8 and AT180 antibodies, was about one-tenth of that deposited in EOAD. Because the cases were matched for age at onset and duration of disease, it is unlikely that these differences in tau load reflect demographic variations or differences in stage of the disease at death. Indeed, there were no correlations between tau load and duration of illness for any of the disease groups. However, because, in AD at least [46,47], tau proteins are incorporated into aggregated filamentous structures on a whole molecule basis, and not as a series of (variably) truncated molecules, it might be argued that variations in tau load between disorders using these two antibodies reflect differences in degree of phosphorylation of tau at different epitopes, or ease of antibody accessibility, rather than actual number of tau molecules present. These considerations are unlikely to explain the very high differences in tau load between FTLD and EOAD with AT8 antibody at least, because biochemical measures of insoluble tau load by Western blot using this particular antibody have also shown much greater quantities of insoluble tau within the brain in AD compared with FTLD cases (Hasegawa, unpub. data). Present data suggest therefore that there is a lower accumulation of pathological tau over the span of the illness in the brains of patients with FTLD, irrespective of underlying cause, compared with those with AD. The reason for this lower tissue accumulation of tau lies mostly with differing anatomical compartmentalization. In AD the pathological tau deposits are present within neuronal cell bodies (as NFT), dendrites (as neuropil threads) and in axon terminals in neuritic plaques. Tau load in AD, as measured here, represents the composite total of these three anatomical compartments. However, in FTDP-17, and in FTLD with Pick bodies, the bulk of the pathological tau is perikaryal, with little neuropil staining in most instances, except as above where there may be additional glial tau or neuritic plaques present.

The results obtained with AT100 antibody are interesting. AT100 labels pathological aggregations of the PHF in NFT in AD, but does not label normal tau [43]. This antibody detects phosphorylated epitopes Thr212/Ser214 in PHF with the epitope being achieved by the sequential phosphorylation of tau at Thr212 by GSK-3β, then at Ser214 by protein kinase A (PKA) in the presence of polyanions such as heparin and tRNA [48]. In this present study, there was little or no immunoreactivity with AT100 in cases of FTLD with Pick bodies, in contrast to cases of AD and FTDP-17. This suggests that in FTLD with Pick bodies either the requirements needed for the formation of the AT100 epitope [48] are not fulfilled, and the epitope is therefore not phosphorylated, or that the tertiary structure of tau in Pick bodies upon fixation makes the epitope inaccessible even though it may be phosphorylated. Maillot and co-workers [49] have detected, by Western blot, insoluble tau in brain tissue of cases of FTLD with Pick bodies using AT100, implying that this epitope is indeed phosphorylated, and that changes in the conformational structure of Pick bodies on tissue fixation may be masking the AT100 epitope. This is quite possible, because low or no Pick body immunoreactivity has been observed with another phosphorylation-dependent antibody, 12E8, raised against the Ser262 epitope [37,50]. However, in this instance, it was also not possible, using 12E8, to detect tau proteins from FTLD cases with Pick bodies on Western blotting [49], implying that a non-phosphorylation of this particular epitope is responsible for the lack of detection of tau in Pick bodies. In AD [51] and *MAPT* exon 10 +16 [34,37] cases, 12E8 specifically stains well-formed NFT rather than pretangles; AT100, likewise, stains NFT strongly, and pretangles less strongly [43]. Nonetheless, in another study, Ferrer and colleagues used a different (to 12E8) antibody against Ser262 epitope (Ser^{262}), which in AD stains pretangles, and showed Pick bodies to be strongly reactive [52]. Hence, the reason for the lack of Pick body staining with AT100 is still not clear.

Also of particular note are findings in *MAPT* P301L mutation where AT100 antibody stained tau aggregations much more strongly than the other two antibodies, in contrast to other *MAPT* mutations where AT8 was usually strongest (see Figure 1). It is therefore possible that protein conformational changes induced by this mutation may help to fulfil the requirements for formation of the Thr212/Ser214 epitope [48]. However, the Ser202 (AT8) epitope needs to be phosphorylated before formation of the AT100 epitope [48], yet in P301L mutation AT8 immunoreactivity was less than that of AT100. This suggests that conformational changes of tau protein, potentially induced by P301L mutation, confer a lesser accessibility of the AT8 antibody to its epitope, which although phosphorylated is relatively undetected, while in contrast such changes enhance the detection of the AT100 Thr212/Ser214 epitope.

On face value, present findings might therefore suggest that FTLD is a pathologically 'less aggressive' illness than AD. Because there is greater tissue loss in FTLD than in AD, it might be argued that the accumulation of aggregated tau proteins within neurones in FTLD is incidental and epiphenomenal to the main disease process that leads to the gross neurodegeneration seen in these cases. However, it may also be the case that *MAPT* mutations cause changes in cellular function so lethal to the nerve cell that death occurs before (many of) the cells can accumulate (much) tau. One direct effect of the *MAPT* missense mutations leads to formation of mutated tau molecules that lose ability to bind microtubules and reduce microtubule assembly resulting in impaired axonal transport [22]. Exon 10 mutations increase the ratio between 4R : 3R tau and perturb the precisely regulated stoichiometric binding of tau proteins to tubulin needed for microtubule assembly [53]. Hence, catastrophic disruption in protein transport leading to cell death may occur in many neurones without significant tau accumulation having taken place.

It has been shown that unpolymerized hyperphosphorylated tau proteins in the cell cytosol can sequester normal functional tau, forming filaments and leading to inhibition and disassembly of microtubules [54]. However, polymerized tau in the form of PHF does not possess this ability [55]. In AD, neurones may therefore 'promote' PHF formation from hyperphosphorylated tau in order to protect normal cytosolic tau from being sequestered into filaments, thereby allowing cells to survive longer [56]. Because tau in AD is neither mutated nor produced in a stoichiometrically unbalanced way, it is possible therefore that microtubule formation and function can be maintained (longer than in FTLD) despite the accumulation of PHF. Tau aggregation may therefore be a protective or an adaptive response of neurones. Due to the catastrophic effect of *MAPT* mutations on microtubule function, this process in FTLD is inefficient or ineffective, and many nerve cells die without ever accumulating (much) tau. Only those (relatively few) nerve cells better able to resist

the cellular effects of the mutation, and to 'package' abnormal tau molecules into aggregates, are able to function for longer. However, even in AD, accumulation of tau as PHF is not without detriment, with progressive loss of endoplasmic reticulum and ribosomes with accumulating PHF [57], indicating a decline in the nerve cell's synthetic machinery that eventually crosses a threshold to continued survival.

In sporadic FTLD with Pick bodies it is presumed that, as in FTDP-17, loss of microtubule function is likewise invoked through post-translational hyperphosphorylation changes in tau, although as yet the precise mechanism underpinning this is not known. Nonetheless, tau deposition is again about 10 times less than that in EOAD and the same mechanistic arguments (as in FTDP-17) for this smaller accumulation of tau may apply.

However, it could also be argued that the lower level of tau accumulated in FTLD compared with AD reflects the relative ease of degradation and clearance in each disorder with more pathological tau being removed from the brain during the course of the illness than is possible in AD. In AD, the hyperphosphorylated tau is assembled into highly insoluble PHF that become heavily modified through processes such as glycation [58]. Certainly, under the electron microscope, tau filaments in FTLD and AD have different ultrastructural appearances. In FTLD, the tau filaments are usually straight (with some twisted filaments) in those *MAPT* mutations in which Pick bodies are present [13], whereas the NFT-like structures in cases with exon 10 and splice mutations are composed of wide flat twisted ribbons [34], not PHF. These latter filamentous types may be more susceptible to degradation both internally and externally than PHF which even after cell death in AD remain largely intact as 'ghost tangles'. However, the lack of excessive tau in R406W mutation (compared with other *MAPT* mutations), where tau is present as PHF [6,21], would argue against this, although the long disease durations present in many patients with this particular mutation (in the three cases studied here disease duration was 7–29 years) suggests an unusually mild pathological phenotype with the low tau levels being a reflection of this. It would be interesting to compare tau loads using antibodies against glycation end-products or anti-tau antibodies like Alz50 and TG-3 which recognize tau only in specific conformations [59].

It might further be argued that even though the frontal cortex contains tau pathology for all three diseases under investigation, this might not be an appropriate or representative brain region to work on in a study of this kind, being affected relatively less than other regions (for example, temporal cortex) at end-stage disease at least as far as AD, and maybe also sporadic FTLD with Pick bodies [60] and FTDP-17 cases with N279K (in which a movement disorder is prominent) [20,23] are concerned. However, because the frontal cortex is not 'saturated' by tau pathology, even at end-stage disease, its study should better allow the relationship between tau deposition and *MAPT* mutation, or disease type, to be determined than would be the case were end-stage 'burnt out' regions like temporal cortex to be examined. The low levels of tau in frontal cortex in FTLD compared with those in AD could reflect declining disease in this region in FTLD, and that there could be regions of the brain in this latter disorder where the disease process is evolving more actively. However, histological examination of the brain in FTLD with respect to tau deposition refutes this where the level of tau deposition declines when moving in an anterior-posterior direction into better preserved regions of (frontal and parietal cortex) [13,34].

One potential weakness of the present study is that we have only employed phosphorylation-dependent tau antibodies and therefore the tau measurements we have obtained with any given antibody might reflect, at least partially, that proportion of tau molecules in which the epitope concerned is accordingly phosphorylated. As mentioned earlier in connection with AT100 immunostaining, different levels of phosphorylation at different epitopes on tau, or antibody accessibility, might explain the variations in mean tau load between antibodies, and between disease groups. In order to determine whether the antibodies we have used here have detected all, or only a proportion of, the insoluble tau pathology, it will be necessary to perform further analysis using a phospho-independent antibody, or to compare insoluble tau loads by biochemical techniques.

In conclusion, we suggest that the amount of insoluble tau deposited within the brain in FTLD does not depend in any systematic way upon the presence, or type, of *MAPT* mutation, or on what physiological change is generated. Furthermore, the brain tau load in FTLD would seem to be considerably less than that in EOAD, and this finding raises important questions relating to the role of aggregated tau in neurodegeneration – whether this represents an adaptive response aimed at promoting survival of neurones, or is indeed a detrimental change which brings about the demize of the affected cell.

Acknowledgements

This study was supported by a Wolfson Scholarship to AMS and Alzheimer's Research Trust Alzheimer's Disease Research Centre Grant to DMAM. The authors wish to thank the many other people who were involved in collecting and characterizing the FTLD cases with *MAPT* mutations, and the other FTLD and EOAD cases, and by doing so making possible this multicentre collaborative study.

References

1 Foster NL, Wilhelmsen K, Sima AA, Jones MZ, D'Amato CJ, Gilman S. Frontotemporal dementia and parkinsonism linked to chromosome 17: a consensus conference. *Ann Neurol* 1997; **41**: 706–15
2 Hutton M, Lendon CL, Rizzu P, Baker M, Froelich S, Houlden H, Pickering-Brown S, Chakraverty S, Isaacs A, Grover A, Hackett J, Adamson J, Lincoln S, Dickson D, Davies P, Petersen RC, Stevens M, de Graaff E, Wauters E, van Baren J, Hillebrand M, Joosse M, Kwon MJ, Nowotny P, Che LK, Norton J, Morris JC, Reed LA, Trojanowski JQ, Basun H, Lannfelt L, Neystat M, Fahn S, Dark F, Tannenberg T, Dodd PR, Hayward N, Kwok JBJ, Schofield PR, Andreadis A, Snowden J, Craufurd D, Neary D, Owen F, Oostra BA, Hardy J, Goate A, van Swieten J, Mann D, Lynch T, Heutink P. Association of missense and 5′-splice-site mutations in tau with the inherited dementia FTDP-17. *Nature* 1998; **393**: 702–5
3 Poorkaj P, Bird TD, Wijsman E, Nemens E, Garruto RM, Anderson L, Andreadis A, Wiederholt WC, Raskind M, Schellenberg GD. Tau is a candidate gene for chromosome 17 frontotemporal dementia. *Ann Neurol* 1998; **43**: 815–25
4 Spillantini MG, Murrell JR, Goedert M, Farlow MR, Klug A, Ghetti B. Mutation in the tau gene in familial multiple system tauopathy with presenile dementia. *Proc Natl Acad Sci USA* 1998; **95**: 7737–41
5 Houlden H, Baker M, Adamson J, Grover A, Waring S, Dickson D, Lynch T, Boeve B, Petersen RC, Pickering-Brown S, Neary D, Crauford D, Snowden JS, Mann D, Hutton M. Frequency of tau mutations in three series of non-Alzheimer's degenerative dementia. *Ann Neurol* 1999; **46**: 243–8
6 Rizzu P, Van Swieten JC, Joosse M, Hasegawa M, Stevens M, Tibben A, Niermeijer MF, Hillebrand M, Ravid R, Oostra BA, Goedert M, van Duijn CM, Heutink P. High prevalence of mutations in the microtubule-associated protein tau in a population study of frontotemporal dementia in the Netherlands. *Am J Hum Genet* 1999; **64**: 414–21
7 Rosso SM, Landweer EJ, Houterman M, Donker Kaat L, van Duijn CM, van Swieten JC. Medical and environmental risk factors for sporadic frontotemporal dementia: a retrospective case-control study. *J Neurol Neurosurg Psychiatry* 2003; **74**: 1574–6
8 Mann DM. The neuropathology and molecular genetics of frontotemporal dementia. In *Dementia*, edition 2nd edn. Eds J O'Brien, D Ames, A Burns. London: Arnold, 2000: 759–68
9 Reed LA, Wszolek ZK, Hutton M. Phenotypic correlations in FTDP-17. *Neurobiol Aging* 2001; **22**: 89–107
10 Murrell JR, Spillantini MG, Zolo P, Guazzelli M, Smith MJ, Hasegawa M, Redi F, Crowther RA, Pietrini P, Ghetti B, Goedert M. Tau gene mutation G389R causes a tauopathy with abundant pick body-like inclusions and axonal deposits. *J Neuropathol Exp Neurol* 1999; **58**: 1207–26
11 Ghetti B, Murrell JR, Zolo P, Spillantini MG, Goedert M. Progress in hereditary tauopathies: a mutation in the Tau gene (G389R) causes a Pick disease-like syndrome. *Ann N Y Acad Sci* 2000; **920**: 52–62
12 Lippa CF, Zhukareva V, Kawarai T, Uryu K, Shafiq M, Nee LE, Grafman J, Liang Y, St George-Hyslop PH, Trojanowski JQ, Lee VM. Frontotemporal dementia with novel tau pathology and a Glu342Val tau mutation. *Ann Neurol* 2000; **48**: 850–8
13 Pickering-Brown SM, Baker M, Yen S-H, Liu W-K, Hasegawa M, Cairns NJ, Lantos PL, Rossor M, Iwatsubo T, Davies Y, Allsop D, Furlong R, Owen F, Hardy J, Mann DMA, Hutton M. Pick's disease is associated with mutations in the *tau* gene. *Ann Neurol* 2000; **48**: 859–67
14 Rizzini C, Goedert M, Hodges JR, Smith MJ, Jakes R, Hills R, Xuereb JH, Crowther RA, Spillantini MG. Tau gene mutation K257T causes a tauopathy similar to Pick's disease. *J Neuropathol Exp Neurol* 2000; **59**: 990–1001
15 Neumann M, Schulz-Schaeffer W, Crowther RA, Smith MJ, Spillantini MG, Goedert M, Kretzschmar HA. Pick's disease associated with the novel Tau gene mutation K369I. *Ann Neurol* 2001; **50**: 503–13
16 Hayashi S, Toyoshima Y, Hasegawa M, Umeda Y, Wakabayashi K, Tokiguchi S, Iwatsubo T, Takahashi H. Late-onset frontotemporal dementia with a novel exon 1 (Arg5His) tau gene mutation. *Ann Neurol* 2002; **51**: 525–30
17 Rosso SM, van Herpen E, Deelen W, Kamphorst W, Severijnen LA, Willemsen R, Ravid R, Niermeijer MF, Dooijes D, Smith MJ, Goedert M, Heutink P, van Swieten JC. A novel tau mutation, S320F, causes a tauopathy with inclusions similar to those in Pick's disease. *Ann Neurol* 2002; **51**: 373–6
18 Hogg M, Grujic ZM, Baker M, Demirci S, Guillozet AL, Sweet AP, Herzog LL, Weintraub S, Mesulam MM, LaPointe NE, Gamblin TC, Berry RW, Binder LI, de Silva R, Lees A, Espinoza M, Davies P, Grover A, Sahara N, Ishizawa T, Dickson D, Yen SH, Hutton M, Bigio EH. The L266V tau mutation is associated with frontotemporal dementia and Pick-like 3R and 4R tauopathy. *Acta Neuropathol* 2003; **106**: 323–36

19 Pickering-Brown SM, Baker M, Nonaka T, Ikeda K, Sharma S, Mackenzie J, Simpson SA, Moore JW, Snowden JS, de Silva R, Revesz T, Hasegawa M, Hutton M, Mann DM. Frontotemporal dementia with Pick-type histology associated with Q336R mutation in the tau gene. *Brain* 2004; **127**: 1415–26
20 Wszolek Z, Pfeiffer RF, Bhatt MH, Schelper RL, Cordes M, Snow BJ, Rodnitsky RL, Wolters EC, Arwert F, Calne DB. Rapidly progressive autosomal dominant Parkinsonism and dementia with pallido-ponto-nigral degeneration. *Ann Neurol* 1992; **32**: 312–20
21 van Swieten JC, Stevens M, Rosso SM, Rizzu P, Joosse M, de Koning I, Kamphorst W, Ravid R, Spillantini MG, Niermeijer M, Heutink P. Phenotypic variation in hereditary frontotemporal dementia with tau mutations. *Ann Neurol* 1999; **46**: 617–26
22 Hasegawa M, Smith MJ, Iijima M, Tabira T, Goedert M. FTDP-17 mutations N279K and S305N in tau produce increased splicing of exon 10. *FEBS Lett* 1999; **443**: 93–6
23 Clark LN, Poorkaj P, Wszolek Z, Geschwind DH, Nasreddine ZS, Miller B, Li D, Payami H, Awert F, Markopoulou K, Andreadis A, D'Souza I, Lee VM, Reed L, Trojanowski JQ, Zhukareva V, Bird T, Schellenberg G, Wilhelmsen KC. Pathogenic implications of mutations in the tau gene in pallido-ponto-nigral degeneration and related neurodegenerative disorders linked to chromosome 17. *Proc Natl Acad Sci USA* 1998; **95**: 13103–7
24 Bugiani O, Murrell JR, Giaccone G, Hasegawa M, Ghigo G, Tabaton M, Morbin M, Primavera A, Carella F, Solaro C, Grisoli M, Savoiardo M, Spillantini MG, Tagliavini F, Goedert M, Ghetti B. Frontotemporal dementia and corticobasal degeneration in a family with a P301S mutation in tau. *J Neuropathol Exp Neurol* 1999; **58**: 667–77
25 Delisle MB, Murrell JR, Richardson R, Trofatter JA, Rascol O, Soulages X, Mohr M, Calvas P, Ghetti B. A mutation at codon 279 (N279K) in exon 10 of the Tau gene causes a tauopathy with dementia and supranuclear palsy. *Acta Neuropathol* 1999; **98**: 62–77
26 D'Souza I, Poorkaj P, Hong M, Nochlin D, Lee VM, Bird TD, Schellenberg GD. Missense and silent tau gene mutations cause frontotemporal dementia with parkinsonism-chromosome 17 type, by affecting multiple alternative RNA splicing regulatory elements. *Proc Natl Acad Sci USA* 1999; **96**: 5598–603
27 Goedert M, Spillantini MG, Crowther RA, Chen SG, Parchi P, Tabaton M, Lanska DJ, Markesbery WR, Wilhelmsen KC, Dickson DW, Petersen PB, Gambetti P. Tau gene mutation in familial progressive subcortical gliosis. *Nat Med* 1999; **5**: 454–7
28 Mirra SS, Murrell JR, Gearing M, Spillantini MG, Goedert M, Crowther RA, Levey AI, Jones R, Green J, Shoffner JM, Wainer BH, Schmidt ML, Trojanowski JQ, Ghetti B. Tau pathology in a family with dementia and a P301L mutation in tau. *J Neuropathol Exp Neurol* 1998; **58**: 335–45
29 Nasreddine ZS, Loginov M, Clark LN, Lamarche J, Miller BL, Lamontagne A, Zhukareva V, Lee VM, Wilhelmsen KC, Geschwind DH. From genotype to phenotype, a clinical pathological, and biochemical investigation of frontotemporal dementia and parkinsonism (FTDP-17) caused by the P301L tau mutation. *Ann Neurol* 1999; **45**: 704–15
30 Arima K, Kowalska A, Hasegawa M, Mukoyama M, Watanabe R, Kawai M, Takahashi K, Iwatsubo T, Tabira T, Sunohara N. Two brothers with frontotemporal dementia and parkinsonism with an N279K mutation of the tau gene. *Neurology* 2000; **54**: 1787–95
31 Spillantini MG, Yoshida H, Rizzini C, Lantos PL, Khan N, Rossor MN, Goedert M, Brown J. A novel tau mutation (N296N) in familial dementia with swollen achromatic neurons and corticobasal inclusion bodies. *Ann Neurol* 2000; **48**: 939–43
32 Stanford PM, Halliday GM, Brooks WS, Kwok JB, Storey CE, Creasey H, Morris JG, Fulham MJ, Schofield PR. Progressive supranuclear palsy pathology caused by a novel silent mutation in exon 10 of the tau gene: expansion of the disease phenotype caused by tau gene mutations. *Brain* 2000; **123**: 880–93
33 Iseki E, Matsumura T, Marui W, Hino H, Odawara T, Sugiyama N, Suzuki K, Sawada H, Arai T, Kosaka K. Familial frontotemporal dementia and parkinsonism with a novel N296H mutation in exon 10 of the tau gene and a widespread tau accumulation in the glial cells. *Acta Neuropathol* 2001; **102**: 285–92
34 Pickering-Brown SM, Richardson AM, Snowden JS, McDonagh AM, Burns A, Braude W, Baker M, Liu WK, Yen SH, Hardy J, Hutton M, Davies Y, Allsop D, Craufurd D, Neary D, Mann DM. Inherited frontotemporal dementia in nine British families associated with intronic mutations in the tau gene. *Brain* 2002; **125**: 732–51
35 Grover A, DeTure M, Yen SH, Hutton M. Effects on splicing and protein function of three mutations in codon N296 of tau in vitro. *Neurosci Lett* 2002; **323**: 33–6
36 Halliday GM, Song YJC, Creasey H, Morris JG, Brooks WS, Kril JJ. Neuropathology in the S305S tau gene mutation. *Brain* 2006 (in press)
37 Taniguchi S, McDonagh AM, Pickering-Brown SM, Umeda Y, Iwatsubo T, Hasegawa M, Mann DM. The neuropathology of frontotemporal lobar degeneration with respect to the cytological and biochemical characteristics of tau protein. *Neuropathol Appl Neurobiol* 2004; **30**: 1–18
38 Mirra SS, Heyman A, McKeel D, Sumi SM, Crain BJ, Brownlee LM, Vogel FS, Hughes JP, van Belle G, Berg L. The Consortium to Establish a Registry for Alzheimer's Disease (CERAD). Part II. Standardization of the neuropathologic assessment of Alzheimer's disease. *Neurology* 1991; **41**: 479–86
39 Braak H, Braak E. Neuropathological stageing of Alzheimer-related changes. *Acta Neuropathol* 1991; **82**: 239–59
40 Kertesz A, McGonagle P, Blair M, Davidson W, Munoz DG. The evolution and pathology of frontotemporal dementia. *Brain* 2005; **128**: 1996–2005

41 McKhann GM, Albert MS, Grossman M, Miller B, Dickson D, Trojanowski JQ. Workgroup on Frontotemporal dementia and Picks disease. Clinical and pathological diagnosis of frontotemporal dementia: report of the workgroup on Frontotemporal dementia and Picks disease. *Arch Neurol* 2001; **59**: 1203–4

42 Goedert M, Jakes R, Crowther RA, Six J, Lubke U, Vandermeeren M, Cras P, Trojanowski JQ, Lee VM. The abnormal phosphorylation of tau protein at Ser-202 in Alzheimer disease recapitulates phosphorylation during development. *Proc Natl Acad Sci USA* 1993; **90**: 5066–70

43 Mercken M, Vandermeeren M, Lubke U, Six J, Boons J, Van de Voorde A, Martin JJ, Gheuens J. Monoclonal antibodies with selective specificity for Alzheimer Tau are directed against phosphatase-sensitive epitopes. *Acta Neuropathol* 1992; **84**: 265–72

44 Goedert M, Jakes R, Crowther RA, Cohen P, Vanmechelen E, Vandermeeren M, Cras P. Epitope mapping of monoclonal antibodies to the paired helical filaments of Alzheimer's disease: identification of phosphorylation sites in tau protein. *Biochem J* 1994; **301**: 871–7

45 Mann DM, McDonagh AM, Pickering-Brown SM, Kowa H, Iwatsubo T. Amyloid beta protein deposition in patients with frontotemporal lobar degeneration: relationship to age and apolipoprotein E genotype. *Neurosci Lett* 2001; **304**: 161–4

46 Kondo J, Honda T, Mori H, Hamada Y, Miura R, Ogawara M, Ihara Y. The carboxyl third of tau is tightly bound to paired helical filaments. *Neuron* 1988; **1**: 827–34

47 Kosik KS, Orecchio LD, Binder L, Trojanowski JQ, Lee VM, Lee G. Epitopes that span the tau molecule are shared with paired helical filaments. *Neuron* 1988; **1**: 817–25

48 Zheng-Fischhofer Q, Biernat J, Mandelkow EM, Illenberger S, Godemann R, Mandelkow E. Sequential phosphorylation of Tau by glycogen synthase kinase-3β and protein kinase A at Thr212 and Ser214 generates the Alzheimer-specific epitope of antibody AT100 and requires a paired-helical-filament-like conformation. *Eur J Biochem* 1998; **252**: 542–52

49 Mailliot C, Sergeant N, Bussiere N, Caillet-Boudin ML, Delacourte A, Buee L. Phosphorylation of specific sets of tau isoforms reflects different neurofibrillary degeneration processes. *FEBS Lett* 1998; **433**: 201–4

50 Probst A, Tolnay M, Langui D, Goedert M, Spillantini MG. Pick's disease: hyperphosphorylated tau protein segregates to the somatoaxonal compartment. *Acta Neuropathol* 1996; **92**: 588–96

51 Augustinack JC, Schneider A, Mandelkow EM, Hyman BT. Specific tau phosphorylation sites correlate with severity of neuronal cytopathology in Alzheimer's Disease. *Acta Neuropathol* 2002; **103**: 26–35

52 Ferrer L, Barrachina M, Puig B. Anti-tau phosphospecific Ser^{262} antibody recognises a variety of abnormal hyperphosphorylated tau deposits in tauopathies including Pick bodies and argyrophilic grains. *Acta Neuropathol* 2002; **104**: 658–64

53 Goedert M, Spillantini MG, Cairns NJ, Crowther RA. Tau proteins of Alzheimer paired helical filaments: abnormal phosphorylation of all six brain isoforms. *Neuron* 1992; **8**: 159–68

54 Alonso AC, Grundke-Iqbal I, Iqbal K. Alzheimer's disease hyperphosphorylated tau sequesters normal tau into tangles of filaments and disassembles microtubules. *Nat Med* 1996; **2**: 783–7

55 Alonso AC, Mederlyova A, Novak M, Grundke-Iqbal I, Iqbal K. Promotion of hyperphosphorylation by frontotemporal dementia tau mutations. *J Biol Chem* 2004; **279**: 34873–81

56 Iqbal K, Alonso Adel C, Chen S, Chohan MO, El-Akkad E, Gong CX, Khatoon S, Li B, Liu F, Rahman A, Tanimukai H, Grundke-Iqbal I. Tau pathology in Alzheimer disease and other tauopathies. *Biochim Biophys Acta* 2005; **1739**: 198–210

57 Sumpter PQ, Mann DMA, Davies CA, Yates PO, Snowden JS, Neary D. An ultrastructural analysis of the effects of accumulation of neurofibrillary tangle in pyramidal cells of the cerebral cortex in Alzheimer's disease. *Neuropathol Appl Neurobiol* 1986; **12**: 305–19

58 Smith MA, Siedlak SL, Richey PL, Nagaraj RH, Elhammer A, Perry G. Quantitative solubilization and analysis of insoluble paired helical filaments from Alzheimer disease. *Brain Res* 1996; **717**: 99–108

59 Jicha GA, Lane E, Vincent I, Otvos L Jr, Hoffmann R, Davies P. A conformation- and phosphorylation-dependent antibody recognizing the paired helical filaments of Alzheimer's disease. *J Neurochem* 1997; **69**: 2087–95

60 Wechsler AF, Verity MA, Rosenschein S, Fried I, Scheibel AB. Pick's disease. A clinical, computed tomographic, and histologic study with golgi impregnation observations. *Arch Neurol* 1982; **39**: 287–90

Received 12 September 2005
Accepted after revision 24 January 2006

Cerebral networks for spontaneous and synchronized singing and speaking

Yoko Saito[a,b,c], Kenji Ishii[b], Kazuo Yagi[c], Itaru F. Tatsumi[d] and Hidehiro Mizusawa[a]

[a]Department of Neurology and Neurological Science, Tokyo Medical and Dental University, [b]Positron Medical Center, Tokyo Metropolitan Institute of Gerontology, [c]Department of Radiological Science, Tokyo Metropolitan University of Health Sciences and [d]Language, Cognition and Brain Science Research Group, Tokyo Metropolitan Institute of Gerontology, Tokyo, Japan

Correspondence and requests for reprints to Kenji Ishii, MD, Positron Medical Center, Tokyo Metropolitan Institute of Gerontology, 1-1 Nakacho, Itabashi-ku, Tokyo 173-0022, Japan
Tel: +81 3 3964 3241 ext. 3503; fax: +81 3 3964 2188; e-mail: ishii@pet.tmig.or.jp

Received 8 September 2006; accepted 26 September 2006

Singing in unison is usually easier than singing alone, but the neural mechanism underlying these two contrasting modes of singing remains unknown. We investigated neural correlates of singing by a functional magnetic resonance imaging study focusing on the capacities of spontaneity and synchronization and compared them with those of speaking. The left inferior frontal gyrus appears important for self-generation of text in singing and speaking without auditory input, whereas the left posterior planum temporale plays a key role in synchronizing both text and melody, in combination with the bilateral inferior parietal lobule for singing along, and with the left angular gyrus for speaking in chorus. These findings indicate that text and melody are not processed symmetrically or parallel in singing a well-learned song. *NeuroReport* 17:1893–1897 © 2006 Lippincott Williams & Wilkins.

Keywords: functional magnetic resonance imaging, inferior frontal gyrus, planum temporale, singing, speaking, spontaneity, synchronization

Introduction

When singing, we occasionally sing alone; often, however, we sing along with others. This singing may or may not be accompanied by instrumental music. Similarly, although we usually speak alone, we occasionally speak together in a group, for example, during group chanting. Neural networks for singing should involve control mechanisms of two contrasting modes: self-production and synchronized production. It is essential for the self-production of a song to retrieve and represent the internally stored lyrics, rhythm, and melody without the help of external sensory information. On the other hand, it is important for the synchronized production of a song to monitor the external auditory information and to concurrently render synchronous control of articulation. In terms of simple voluntary movements such as finger tapping, there have been several reports that have focused on the differences in the central mechanisms for self-paced movements and externally cued movements [1]. Recently, investigations have been conducted on more complex tasks of finger tapping to external auditory rhythms, such as synchronization compared with syncopation [2], and finger tapping following various rhythms [3]. This work aroused an interest in auditory–motor correlations rather than the spontaneous control of voluntary movements. No previous studies have been found focusing on the capacities of spontaneity and synchronization for singing. It may be useful to investigate the neural mechanism underlying singing from the standpoint of spontaneity and synchronization for the planning of therapy for apraxia of speech, aphasia, and dementia [4]. The purpose of this study was to investigate the neural mechanisms underlying the two different modes of singing: singing alone and singing along. In this paper, we use the term 'spontaneous' singing to refer to the self-production of a well-learned song without the help of external sensory information, and it does not imply any improvisational behavior.

Some recent works have investigated the neural networks from the viewpoint of simple pitch and melody generation [5,6]. Most of the previous studies that investigated singing, however, showed contrasting mechanisms for language and music [7,8]. These studies have shown a symmetric view of language and music: the inferior frontal gyrus, anterior insula, and superior temporal gyrus in the right hemisphere play a predominant role in singing, whereas the homologous regions in the left hemisphere are mainly involved in speaking. On the basis of a conventional model of cerebral lateralization, some lesion studies have indicated that language and music are dealt with parallel networks [9,10]. On the other hand, behavioral experiments and recent neuroimaging studies have suggested that processes for language and music are not completely separate [11–15]. The complete viewpoint of the inter-relationship between text and melody processing in singing remains unknown. To elucidate the neural correlates underlying spontaneous and synchronized processes in singing, we contrasted them with those in speaking in order to address the issue of integration and segregation of music and language in singing.

Materials and methods

Participants

We studied 20 normal right-handed Japanese nonmusicians (19–24 years old; 10 men and 10 women) without any neurological or hearing impairment, after obtaining their

written informed consent. None had experienced any specific training for singing or playing an instrument, except for ordinary schoolwork. Most of them regularly listened to music, but sang only occasionally in day-to-day life. This study was approved by the Ethics Committee of the Tokyo Metropolitan University of Health Sciences.

Experimental paradigm and stimuli

The task design consisted of the following conditions: (i) overtly singing 'Umi' (The Sea) – a very popular song among the Japanese – alone (Sg_solo); (ii) overtly singing Umi in synchronization with the auditory presentation of the song, including the melody and lyrics (Sg_syn); (iii) listening to the singing undertaken in the previous task (L_Sg); (iv) overtly reciting alone the lyrics of Umi without the melody (Sp_solo); (v) overtly reciting Umi along with an auditory presentation of the lyrics (Sp_syn); (vi) listening to the reciting undertaken in the previous task (L_Sp); and (vii) rest condition. The processes involved in each task are summarized in Table 1. For the participants, it was easy to not only sing the song, but also recite the lyrics because the lyrics had a seven-and-five syllable meter, a characteristic style observed in traditional Japanese poems. The auditory stimuli (sampling rate, 44.1 kHz) of singing and speaking were recorded by a female singer, without adding any effect. The averaged rate, fundamental frequency (F0), and intensity of the auditory stimuli were recorded (mean $\pm$ SD) to be 1.60 ± 0.14 moras/s, 221 ± 43 Hz, and 69.9 ± 8.1 dB SPL (SPL: sound pressure level), respectively, for singing, and 2.5 ± 0.13 moras/s, 215 ± 43 Hz, and 69.9 ± 6.5 dB SPL, respectively, for speaking. The rate of presentation alone was significantly different between singing and speaking ($P < 0.01$, paired t-test). In the sound-proof room, the participants underwent prescan training. During training, they practiced singing synchronously with an auditory presentation (Sg_syn task), and this was done until they sang the entire song correctly by themselves without making any mistakes in the lyrics, melody, rhythm and tempo, as assessed by the examiner. Prescan training for the speaking version was also done in the same way.

Data acquisition

Magnetic resonance imaging (MRI) data acquisition was performed with a 1.5-T scanner (Signa; General Electric, Milwaukee, Wisconsin) by using a gradient-echo echoplanar imaging-sequence (TR, 5000 ms; TE, 35.1 ms; flip angle, 60°; matrix size, 128×128; field of view, 24×24 cm^2; and 21 slices with 5 mm thickness). The functional MRI procedure involved six runs that were labeled Sg_solo, Sg_syn, L_Sg, Sp_solo, Sp_syn, and L_Sp and the order was counterbalanced across the participants. One run consisted of six blocks in which the rest block (60 s) alternated with the task block (60 s), and the six runs were performed at 5-min intervals. The participants gently bit disposable wooden bite-bars with their molars during scanning to minimize head and jaw motion artifacts associated with articulation, but the articulation was intelligible. During the scan, the performance of the participant was monitored for text and melody components by experimenters. After each scan, we asked the participants whether they could hear the auditory input and their own song/speech clearly during the scan and if they could perform the task as instructed.

Data analysis

Analysis of the functional MRI data was performed using SPM99 (Wellcome Department of Cognitive Neurology, University College London, London, UK) implemented on MATLAB (Mathworks, Natick, Massachusetts, USA). After

Table 1 Components involved in each task

Components		Articulation; self-monitoring		External perception		Spontaneous production		Synchronized production	
Task		Text	Melody	Text	Melody	Text	Melody	Text	Melody
Spontaneous singing: Sg_solo		O	O	-	-	O	O	-	-
Synchronized singing: Sg_syn		O	O	O	O	-	-	O	O
Listening to the song: L_Sg		-	-	O	O	-	-	-	-
Spontaneous speaking: Sp_solo		O	-	-	-	O	-	-	-
Synchronized speaking: Sp_syn		O	-	O	-	-	-	O	-
Listening to the speech: L_Sp		-	-	O	-	-	-	-	-
Paired t-test									
A_1	Sg_solo > Sg_syn								
A_2	Sg_syn > Sg_solo								
B_1	Sp_solo > Sp_syn								
B_2	Sp_syn > Sp_solo								
C_1	Sg_solo > Sp_solo								
C_2	Sg_syn > Sp_syn								
D_1	Sp_solo > Sg_solo								
D_2	Sp_syn > Sg_syn								

Circles indicate that the task includes the component, whereas dashes indicate the task that does not include the component. Light gray boxes show components related to spontaneous processes, and black boxes show components related to synchronized processes.
Sg_solo, spontaneous singing; Sg_syn, synchronized singing; Sp_solo, spontaneous speaking; Sp_syn, synchronized speaking.

realignment, normalization, and smoothing (full-width at half-maximum, 6 mm), the activated voxels were identified using the general linear model approach [16]. In each participant, a single summary 'contrast' image of a given condition was produced by convolving the images with a standard hemodynamic response function. Next, one-sample *t*-test based on the random effects model was applied contrasting passive listening conditions compared with rest: (L_Sg – rest) and (L_Sp – rest). Then, paired *t*-test was applied contrasting one task condition with another task condition, to determine the brain regions that were specifically activated by each component of the task: (Sg_solo – rest) vs. (Sg_syn – rest), (Sp_solo – rest) vs. (Sp_syn – rest), (Sg_solo – rest) vs. (Sp_solo – rest), and (Sg_syn – rest) vs. (Sp_syn – rest) (Table 1). The specific activations of each paired *t*-test was inclusively masked with the minuend contrast to avoid the detection of pseudo activation caused by deactivation (decrease in signal intensity relative to the rest condition) in the subtrahend contrast [17]. For instance, contrast of (Sg_solo – rest) > (Sg_syn – rest) were inclusively masked by (Sg_solo – rest). The threshold for the pass criterion of the inclusive mask was set to $P<0.001$ (uncorrected). For all statistical comparisons, we used a height threshold of $P<0.05$ (corrected) at the cluster statistics level and a spatial extent of $K=30$ voxels. Montreal Neurologic Institute coordinates were converted to the original coordinate system of Talairach and Tounoux (1988) by Matthew Brett's transformations.

Results

At the postscan interview, all participants reported that they could hear their own song/speech and the auditory input of singing/speaking clearly during the scan. In the passive listening tasks, the L_Sg activated the bilateral Heschl's gyrus, bilateral upper bank of the superior temporal sulcus, bilateral posterior part of the planum temporale, left planum polare, right dorsal premotor cortex, and right supplementary motor area, whereas the L_Sp activated the bilateral Heschl's gyrus, bilateral superior temporal sulcus, left posterior planum temporale, and right planum polare.

Specific activations for spontaneous processes and for synchronized processes in singing and speaking are summarized in Table 2a and displayed in Fig. 1. Specific activations for singing processes and for speaking processes in spontaneous and synchronized conditions are summarized in Table 2b. No significant activated area that was involved in speaking but not in singing (D_1 and D_2) existed.

Discussion

The spontaneous tasks selectively activated the left inferior frontal gyrus in contrast to the synchronized tasks: the left anterolateral part of the inferior frontal gyrus in singing and the left pars triangularis of the inferior frontal gyrus in speaking. On the basis of our task design, it can be interpreted that the activation in the left pars triangularis of the inferior frontal gyrus in speaking is specific to the spontaneous generation of text, but it is also possible that

Table 2a Activations for spontaneity and synchronization in each singing and speaking

Brain regions		Singing (Fig. 1a)				Speaking (Fig. 1b)			
		x	*y*	*z*	Z-value	*x*	*y*	*z*	Z-value
Spontaneous process (green)			Sg_solo > Sg_syn				Sp_solo > Sp_syn		
Anterolateral part of the IFG	L	−32	37	−5	4.72				
Pars triangularis of the IFG	L					−42	25	1	4.61
Synchronized process (red)			Sg_syn > Sg_solo				Sp_syn > Sp_solo		
Posterior planum temporale	L	−44	−36	12	5.12	−48	−33	2	5.26
	R	40	−33	10	4.58				
Anterior edge of the IPL	L	−54	−27	21	4.73				
	R	50	−20	24	4.68				
Angular gyrus	L					−56	−49	25	4.93

Sg_solo, spontaneous singing; Sg_syn, synchronized singing; Sp_solo, spontaneous speaking; Sp_syn, synchronized speaking; IFG, inferior frontal gyrus; IPL, inferior parietal lobule.

Table 2b Activations for singing and speaking in each spontaneity and synchronization

Brain regions		Spontaneous process				Synchronized process			
		x	*y*	*z*	Z-value	*x*	*y*	*z*	Z-value
Singing process			Sg_solo > Sp_solo				Sg_syn > Sp_syn		
Dorsal premotor cortex	R	50	12	36	4.79	50	2	40	5.01
IFG/Anterior insula	R	45	29	−5	4.62	40	23	−5	4.64
Anterior cingulate cortex	R	2	23	36	4.02	2	17	34	4.55
Planum temporale	R	52	−22	6	5.16	60	−29	11	4.97
Planum polare	R					48	−4	10	4.42
Middle insula	R					46	2	−3	4.83
Anterior edge of the IPL	L					−50	−22	26	4.34
Speaking process			Sp_solo > Sg_solo NS				Sp_syn > Sg_syn NS		

Talairach coordinates and the Z-values of peak activation; activated regions detected by paired t-test: $P<0.05$ corrected for multiple comparisons, using an inclusive mask: $P<0.001$, uncorrected.
Sg_solo, spontaneous singing; Sg_syn, synchronized singing; Sp_solo, spontaneous speaking; Sp_syn, synchronized speaking; IFG, inferior frontal gyrus; IPL, inferior parietal lobule; L, left; R, right.